Global Journals LaTeX JournalKaleidoscope™
Artificial Intelligence formulated this projection for compatibility purposes from the original article published at Global Journals. However, this technology is currently in beta. *Therefore, kindly ignore odd layouts, missed formulae, text, tables, or figures.*

Numerical Simulation of Vertical Axis Wind Turbine at Low Speed Ratios

Vladimir CardoA[1] and Ion Malael[2]

[1] Gh. Mihoc-C. Iacoba Institute of Mathematical Statistics and Applied Mathematics, Bucharest, Romania

Received: 13 December 2013 Accepted: 4 January 2014 Published: 15 January 2014

Abstract

A renewed interest in vertical axis wind turbines (VAWT) has been seen recently, in particular at relatively low Reynolds number (Rec ? 10 5) appropriate to the urban applications. From this perspective, the Computational Fluid Dynamics (CFD) is regarded as a promising technique for aerodynamic studies of VAWT. The paper presents a computational investigation on a particular dynamic stall phenomenon associated with unsteady flow around the NACA 0018 a irfoil o f a t hree s traight b laded rotor, a t h igh a ngle o f attack (AOA). Two airfoil flows with angle of attack higher than 45o of an isolated blade and a confined blade in rotor at low speed ratios (TSR), are numerically simulated using CFD. It is concluded that the quasi-steady prediction used in previous models is in disagreement with experimental and numerical data because the unsteadiness generated by spinning rotor, though very important for the self-starting of VAWT, in the past were ignored.

Index terms— dynamic stalls; low reynolds number, CFD; vawt.

1 Introduction

he depletion of fossil energy resource and global warming trends has lead to the recognition of a low carbon economy as an international strategy for sustainable development. Among several green and renewable energy resources, wind energy has seen a rapid growth worldwide and will play an increasingly important role in the future economy.

Wind turbines are typical devices that convert the kinetic energy of wind into electricity. From the perspective of urban applications, where the wind is very turbulent and unstable with fast changes in direction and velocity, vertical axis wind turbines have several advantages over the widely used horizontal axis wind turbines. However VAWT suffer from many complicate aerodynamic problems, of which dynamic effects are inherent phenomena when they operating at low values of tip speed ratio (TSR) ? <2, and this has a significant impact on their self-start capabilities, i.e. without external assistance. Therefore, it is crucial to have a good understanding of the starting process, in appropriate to the urban applications of VAWT, which remains to this day incomplete.

Traditionally, dynamic stall is a term used to describe the delay in the stall on wings and airfoils that are rapidly pitched with angle of attack, , significantly beyond the static stall angle and normally can generate a substantially larger lift for a short period of time than can be obtained quasi-statically [1], [2]. The VAWT blade operating at ? ? 2 perceives a cyclic variation in the relative wind speed and the angle of attack which is very similar to what would be experienced with a sinusoidal pitching blade in a stationary frame of reference.

On the basis of this similarity the dynamic stall on VAWT blades was investigated using the simpler motion of oscillating airfoils [3]. However at low speed ratios, ? < 2, the motion has both pitch component and plunge component and the blade frequently experiences high angles of attack beyond the stall value.

Particularly at very low TSR that often occurs in the starting process, the maxim AOA is far beyond the stall angle. Therefore a good representation of high AOA flows is essential in the correct prediction of the aerodynamics and VAWT performance.

2 II.

3 Motion and Aerodynamics of Vawt

Figure 1a is a schematic of a straight bladed fixed-pitch VAWT which is the simplest but typical form of the Darrieus type VAWT. Despite the simplicity, its aerodynamic analysis is still quite complex. One feature is that the relative velocities perceived by the blade always change as the blade moves to different azimuth positions. Figure 1b illustrates typical flow velocity around a rotating VAWT blade at a given azimuth angle as well as the aerodynamic forces perceived by the blade. The azimuth angle is set to be 0 when the blade is at the top at the flight path and it increases in a counter-clock wise direction. It should be noted that, even disregarding the variation of the induced local flow velocity Ulocal, both the magnitude and the direction of the effective velocity perceived by the blade, Ueff, change in a cyclic manner as the blade rotates through different azimuth angles. This kind of motion is called the Darrieus motion [4]. As a result, the aerodynamic loads exerted on the blade change cyclically with ? . Year 2014 I Abstract-A renewed interest in vertical axis wind turbines (VAWT) has been seen recently, in particular at relatively low Reynolds number (Rec ? 10 5) appropriate to the urban applications. From this perspective, the Computational Fluid Dynamics (CFD) is regarded as a promising technique for aerodynamic studies of VAWT. The paper presents a computational investigation on a particular dynamic stall phenomenon associated with unsteady flow around the NACA 0018 airfoil of a three straight bladed rotor, at high angle of attack (AOA). Two airfoil flows with angle of attack higher than 45 o of an isolated blade and a confined blade in rotor at low speed ratios (TSR), are numerically simulated using CFD. It is concluded that the quasi-steady prediction used in previous models is in disagreement with experimental and numerical data because the unsteadiness generated by spinning rotor, though very important for the self-starting of VAWT, in the past were ignored. with their peaks at about same azimuth angle of 90 0 ; unlike these variations, the variations at the low values of ? (? < 2) contain elements of plunging motion and have their peaks at different azimuth angles (130 0 for ? = 1.5) (Fig. 2b).D U or RU ? ? ? ? ?? ?? ? ? ? ? ? ? ?? ? ? ? ? ? ? ? ? ? ? ?? D ? of a blade in ? 2 eff c k U ? ? ? 2 2 cos 1 c k D ? ?? ? ?? ?? ? ? ? ? ? ? D ? max D D ? ?

? This difference is typically termed the phase shift which is an important parameter for generation of thrust.

? The variation of the reduced frequency k shows the existence of a band of tip speed ratios about (0.7 1.5) with the rough increase of frequency like a discontinuity. (Fig. 2c) (0.7 1.5). and ? ? 0.5; commonly this effect is neglected and a quasi-steady assumption is used; ? First level is the located unsteady phenomenon of dynamic stall with lift increment at low angle of attack (? ? 25?), occurring at when and ? ? 2; its effect is similar to a sinusoidal pitching airfoil; ? Second level is the located unsteady phenomenon of dynamic stall with drag reduction at and ? = 0.7-1.5; to this day it is still unknown.

The two types of dynamic stall address to different portions of the static lift characteristic which for the VAWT blades operating at low TSR presents a particular double peak characteristic, with two peak values, C L1S at low AOA and C L2S at high AOA , Fig. 3. The main difference between these two types of stall is dependence upon the Reynolds number: first stall is much dependent on Reynolds and second stall is practically with no-effe on it.

The first phenomenon is a lift dynamic stall similar to airfoils rapidly pitching with the angle of attack ?, significantly beyond the static stall angle, , and normally can generate a substantially larger lift than can be obtained quasi-statically. This phenomenon is well documented [5], [6], and results from the combination of the unsteady motion of the airfoil and the separation of the boundary layer, when the stall process can be divided into four key stages, i. The drag dynamic stall occurs only on blades operating in a closed flow field in which the rotor is acting as a pump on the separated volume of air forcing it to move radially towards the blade.

The drag dynamic stall is a term used to describe the delay in the drop of the second static stall lift coefficient C L2S on the blade passing in the downwind (?=180 0) and which can generate simultaneously little lift and significant drag reduction for a short period of time when TSR is of order unity. The drag stall dynamic stall, occurring at low TSR in the range of ? = 0.7-1.5 (Fig. 2c), characterizes the shift of the operating modes from mixed lift-drag driving to full lift driving which is important for the continuous thrust-producing, i.e. the self-starting of rotor. Therefore, the objective of this paper is to correctly simulate drag dynamic stall which is found in VAWTs and make a contribution towards a better understanding of the flow physics of this unknown phenomenon directly related to the self-starting of VAWT intended for the built and urban environment in the future.

4 III.

5 Cfd Simulations

The CFD simulation of airfoil flow with an AOA higher than 45 o is rarely discussed in the literature. However blades encounter a very high AOA as they rotate at a low TSR (as shown in fig 2a). The aerodynamic data of static airfoil at AOAs ranging from? ? / / 1.0 k c D ? 0 90 ?? ? ? / / 2.0 k c D ? ? ? / / 2.0 k c D ? 0 1 10 S ?? ? ? 0 2 45 S ?? 1S ? a) b) ? ? ? ? Re 80,000;) ;) c L L D a C b C C ?? 0 o to 180 o

is the fundamental input of a double-multiple stream tube (DMS) model that is one widely accepted method for evaluating the power of VAWTs in engineering practice [7]. But, the unsteadiness generated by the rotor operating at low TSR is inevitable in assessment VAWT starting performance. So that, in this section it's contribution due to a confined airfoil into a three straight-bladed rotor is examined and compared with the data from a single static airfoil.

6 a) CFD simulation of single static airfoil

Airfoil NACA 0018 is one of commonly used blade section in VAWTs. In this investigation the aerodynamic data for a full range of AOAs published by Scheldahl and Klimas [8] is used. These experimental high angle of attack (?> 45), occurring at when 0 180 ?? 0 data offer a good opportunity to examine the capacity of CFD at very high AOA's. The commercial CFD software Fluent was employed in flow computational. Fluent is based on the finite volume method which discretizes the computational domain into some small volumes and has been tested in many applications. The detailed computational treatments and algorithms are explained as follows:

i. Mesh geometry and boundary conditions Both O and C-grid mesh topologies can minimize the skewness of a near-wall mesh and converge fast under a high-order discretization scheme. In this study, the O-grid topology was adopted because it can reduce grid number and avoid high aspect ratios of grids in the far wake. In order to resolve the laminar sub layer directly, the first grid spacing on the airfoil was determined to make y + less than 1. Grid-stretching was limited to less than 1.08 in both streamwise and cross flow directions to ensure numerical stability. Figure 4b shows the final mesh in 2D model.

7 ii. Transition Model

The incompressible Navier-Stokes equations are appropriate for solving the VAWT aerodynamics, because the resultant flow velocity is generally smaller than 0.3 times the Mach number. Stall, either static or dynamic, may occur in a rotating VAWT and both are dominated by vortex separation and involve flow unsteadiness. Therefore, an unsteady fluid solver is necessary to investigate such kinds of flow.

The choice of transitional models influences the computational results and the required computation resource. The transition model uses two transport equations, one for intermittency and one for a transition onset criterion in terms of momentum thickness Reynolds number [9].

? transport equation for the intermittency, ?: a b t e R ? ? ? 1 1 2 2 j t jj U P E P E t x t x ? ? ? ? ? ?? ?? ?? ? ?? ? ?? ?? ? ? ? ? ? ? ? ? ? ? ? ?? ?? ? ? ? ? ? ?? ?? ?? ? ? ? ? Re Re Re jt tt t t t j j j U P t x x x ? ?? ?? ? ?? ?? ? ? ? ? ? ? ? ? ? ? ? ?? ? ? ? ? ? ?? ??**(4)**

iii. Simulation setup The 2D Unsteady Reynolds-Averaged Navier-Stokes (URANS) approach was selected to solve the discretized continuity and momentum equation, and a second order implicit formula was used for the temporal discretization. The SIMPLEC scheme was used to solve the pressure-velocity coupling. SIMPLEC converges faster than SIMPLE. Time step size is a crucial parameter in unsteady flow simulations. To get accurate results of an airfoil beyond stall, Sorensen et al. [10] and Travin et al. [11], suggested the non-dimensional time steps to be 0.01 and 0.025 respectively. The dynamic effects of the blade influence the energy extraction process of VAWT, and thus, the determination of the time step should consider amplitude, frequency and far field velocity. In the present study, the reduced frequency was k = 0.24, the physical time step was and the corresponding nondimensional time step was [12].

IV.

8 Results and Discussions

The flow in the VAWT operating at wind speed of 10 m/s was simulated using 2D URANS. Results for a single airfoil blade in high angle of attack flow were compared with the results obtained by a three straightbladed rotor at low TSR.

The CFD simulation of airfoil flow with an AOA higher than 45 o is rarely discussed in the literature where the flow is dominated by the dynamics of the interacting vortices generated by the separating boundary layer. Figure 6a, b shows the pressure field superimposed on the instantaneous streamlines computed for both single blade and three-confined blades. The single airfoil blade in high angle of attack flow produces a different wake structures as the AOA increases, Fig. 6 a. In the near wake there are two main vortices: leading edge vortex (LEV) and trailing edge vortex (TEV). The position of vortices change in terms of the AOA as : when the AOA is ? = 30 o , the LEV is stronger than TEV and this is the last shed vortex (SV) so that the flow produces a classical von Karman vortex street; when the AOA is of order ? ? 45 o , the both LEV and TEV have comparable strengths, SV becomes nearer the airfoil and the flow produce pairs of counter-rotating vortices of equal strengths, called viscous (weak) vortex doublet (VD); and when the AOA exceeds the value ? ? 60 o , noticeably in the flow pattern near the airfoil there are a cluster of the two main vortices and the formation of a quasi-potential (strong) vortex doublet (QPD). Considering Reynolds number circumstances in this study, these vortex structures forming slowly rotating QPD street are perceived as large separation bubbles shedding from the blade. The simulation of the three-straight-bladed rotor reveals another interacting vortex flow which can trigger off the drag dynamic stall phenomenon when the TSR is of order unity. In contrast to the free wake of a single airfoil blade, the closed wake formed in the upwind zone of VAWT is a QPD detaching from the blade due to the flow curvature effect at a certain azimuth angle. After this location, the free QPD strongly interacts with blade and changes the pressure distribution around the airfoil, which has a significant impact on the aerodynamic forces. Drag dynamic stall is an intrinsic feature of blade in Darrieus motion which can be described as a two step process: outset of a vortex doublet structure as the blade approaches its downwind passage (? = 180) when TSR is of order unity followed by the interaction between the separated boundary-layers flow on the suction side of the airfoil and the vortex doublet which shifts inwards due to the flow curvature effect. This features as can be seen in Fig. 6b is well captured by 2D URANS model and a two transport equation transition model.

Figure 6b presents a chronology of the static pressure fields at different azimuth angles ? of a blade in Darrieus motion at ? = 1.0, superimposed on the instantaneous stream lines to depict the complicated vortex structures during the stall process. In the early stage of the upwind phase, a long separation bubble can be detected on the upper surface (here it is not shown , pp the bubble (TSB) which has covered the whole suction surface begins to turn into a VD and at the TSB was completely turn into the VD. At this instance, the VD covers the whole suction surface and C_L is at its maximum value. Further as the blade moves, the VD is degenerated into a concentrating leading edge-vortex (CV), while the weaker trailing edge-vortex is convected away in the downwind movement. At, CV detaches and is come localized in the vicinity of the upper surface of blade. At this instance CD is at its maximum value, after which the drag coefficient drops roughly. The CV moves with the blade in the leeward movement and after the downwind passage ( ) the suction surface switches to opposed side of the blade when the wind favors the convection of the concentrated vortex away from the airfoil, so that the drag dynamic stall ceases and drag increases. This entity embedded in the flow field plays the role of "focus" which squeezes the streamlines around the airfoil when it passes across from upwind to downwind and gradually accelerate flow on the upper surface producing a lower pressure and, thus, the flow around blade behaves like as inviscid one. Therefore, the rough switch of the angle of attack at ? = 1 and ? = 180^0 seen in Fig. 2c, actually becomes a smooth process via blade-vortex wake interaction which has the ability to produce a continuous pressure variation at the downwind passage.

Figure **??** shows the comparison of the lift and drag coefficients from the wind tunnel tests [8], as well as the 2D URANS simulations for a single airfoil blade and three straight-bladed rotor at $Re_c = 10^5$. The over predicted results seen in figure **??** are consistent with the observations found [13], [14] that the 2D models is not adequate for predicting unsteady flow structures with large-scale separations around airfoils at relatively high AOAs. However, the used model does not attempt to model with fidelity the wake vortices, but it is used as a computational tool for the understanding of the different aerodynamic behaviors of airfoils as isolated one and confined other.

When the blade, operating in a Darrieus motion, at , TSR ? 1.0 passes through azimuth angle of 120^0 a vortex doublet structure shifts inwards, interferes with the flow around blade producing a pressure drop along the suction side of airfoil, and the blade is in drag stall, leading to a sudden drop in drag coefficient, see Fig. **??**. With the increase of azimuth angle, the vortex doublet moves away from the suction surface of blade and it is convected in the leeward movement when it is at azimuth angle of 180^0. Further downstream, the flow penetrated from the pressure side of blade into the suction side and the angle of attack began to increase, and therefore a reversed flow occurs at trailing edge, which has a significant impact on the aerodynamic forces, namely the drag coefficient roughly increases during downwind stroke.

Figure 8 shows the tangential force coefficient in terms of azimuth angle and its average value for the three straight-bladed rotor at TSR = 1.0. This positive value indicates the self-starting capability of the Darrieus ? The drag dynamic stall process is triggered by a certain unsteadiness level inside rotor and promotes the shift of operating modes of VAWTs from mixed lift-drag driving to full lift driving, and there by produces the continuous thrust production when TSR exceeds the value one. However, the shift to full lift-driven state is not a guarantee of further acceleration and it is possible the rotor will be locked in the dead band ( ) due to a large area of high angle of attack and insufficient thrust production. In this case others parameters as blade thickness and turbine solidity can be altered for overcoming this drawback.

? Concerning the used computational approach it is remarked that though the 2D URANS model is not adequate for predicting accurately unsteady flow structures with large-scale separation, however, for

? present Rec it is has been able to capture the main features of the drag dynamic stall phenomenon here identified. [1]

[1]© 2014 Global Journals Inc. (US)

1

Figure 1: ?Figure 1 :

1 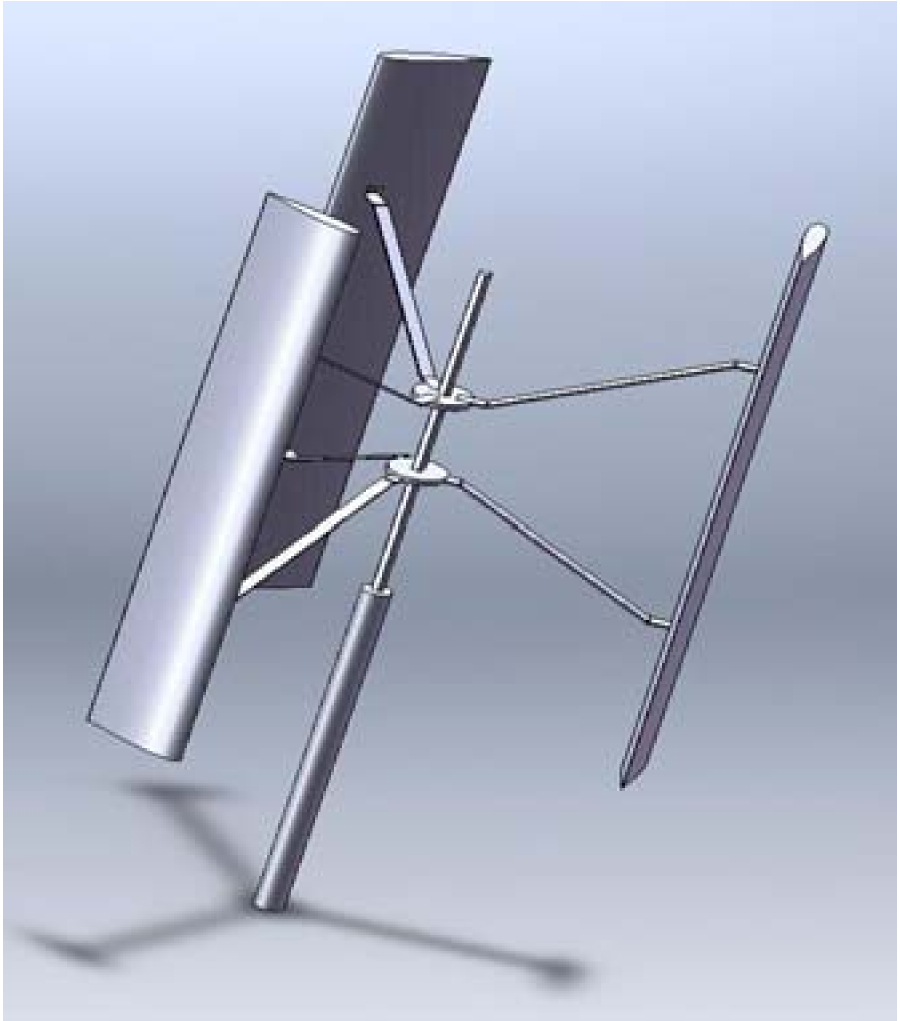

Figure 2: (1)

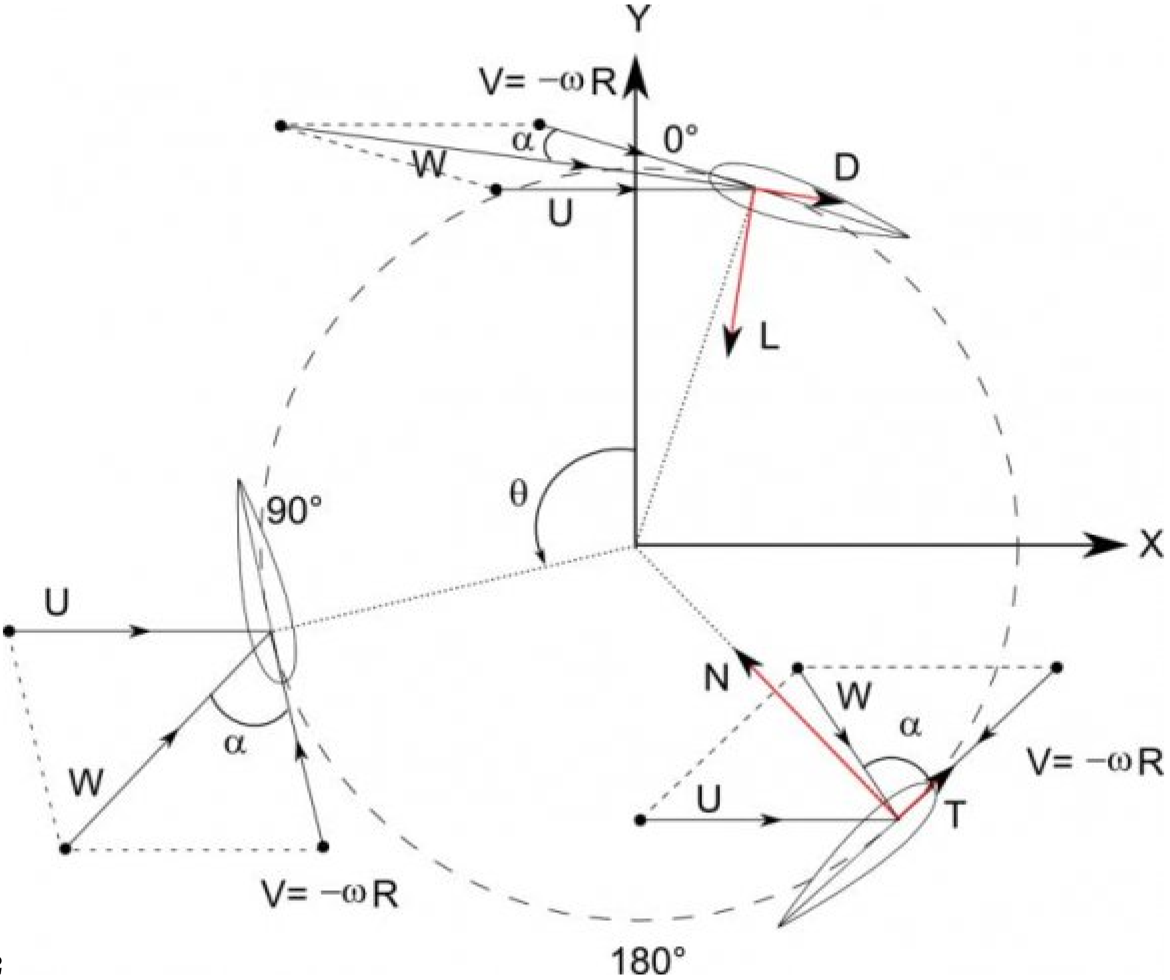

2

Figure 3: Figure 2 :

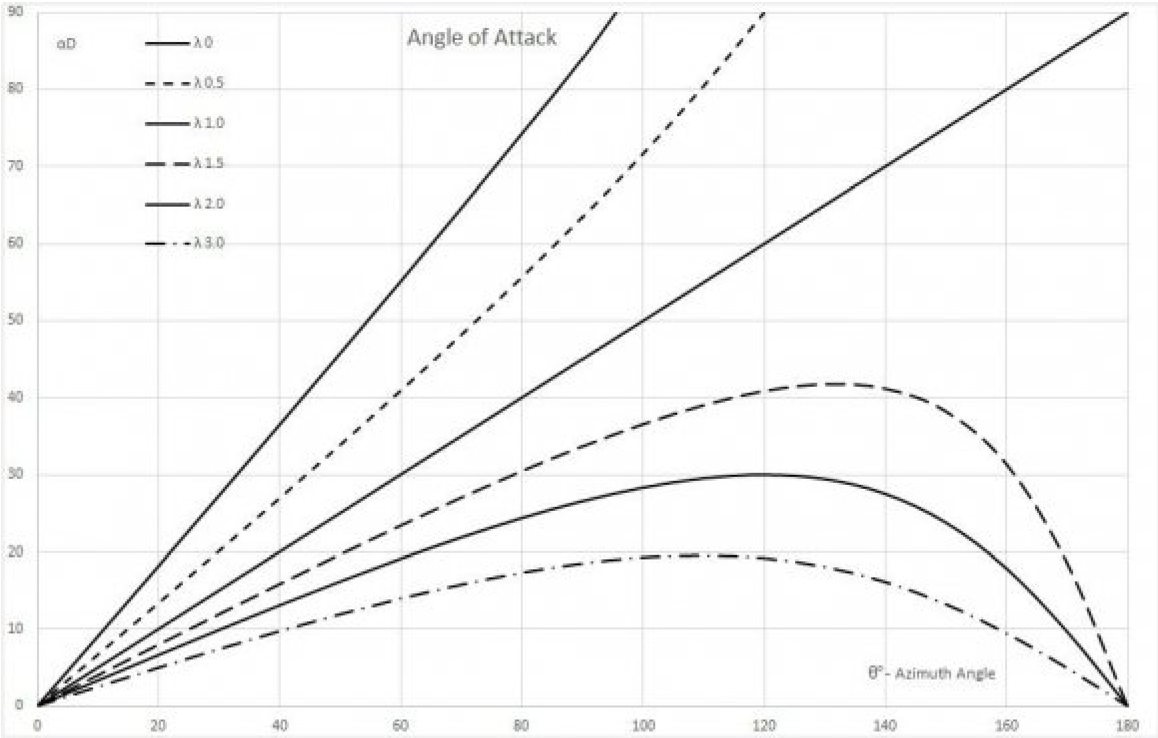

Figure 4:

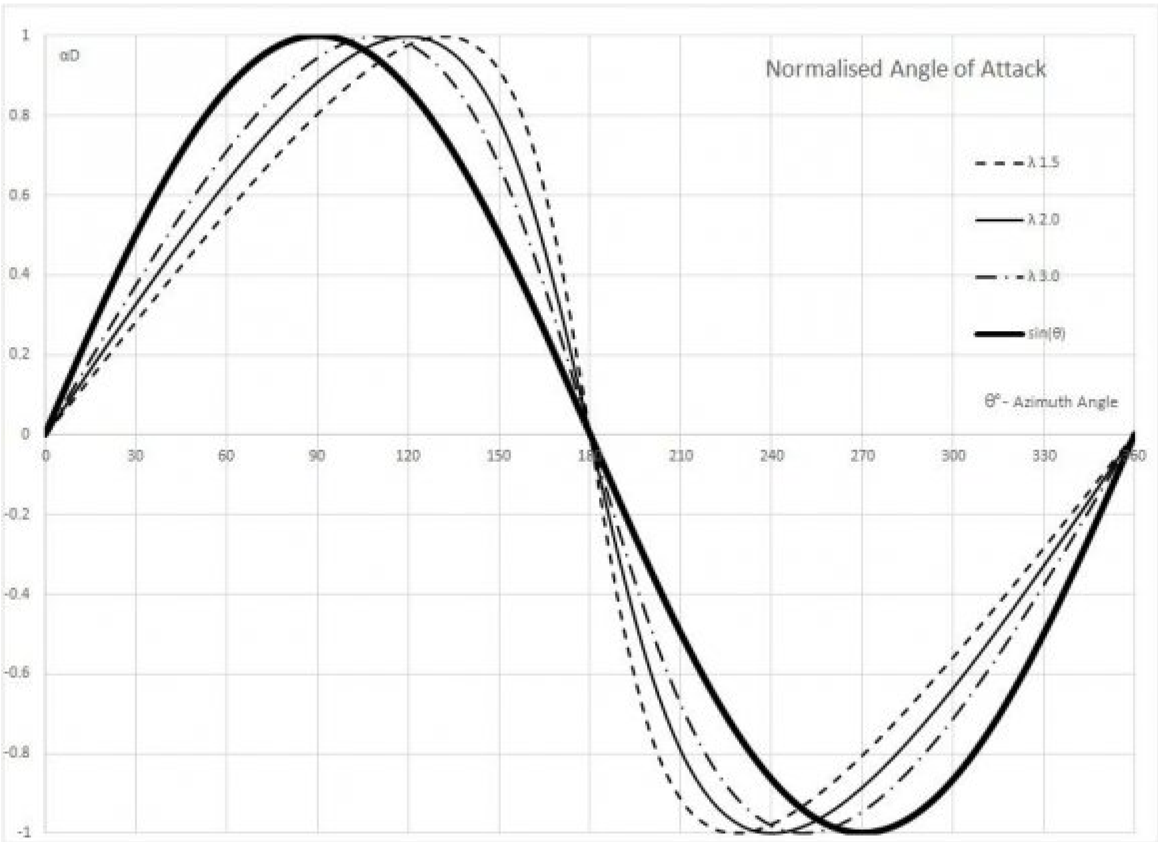

Figure 5:

3

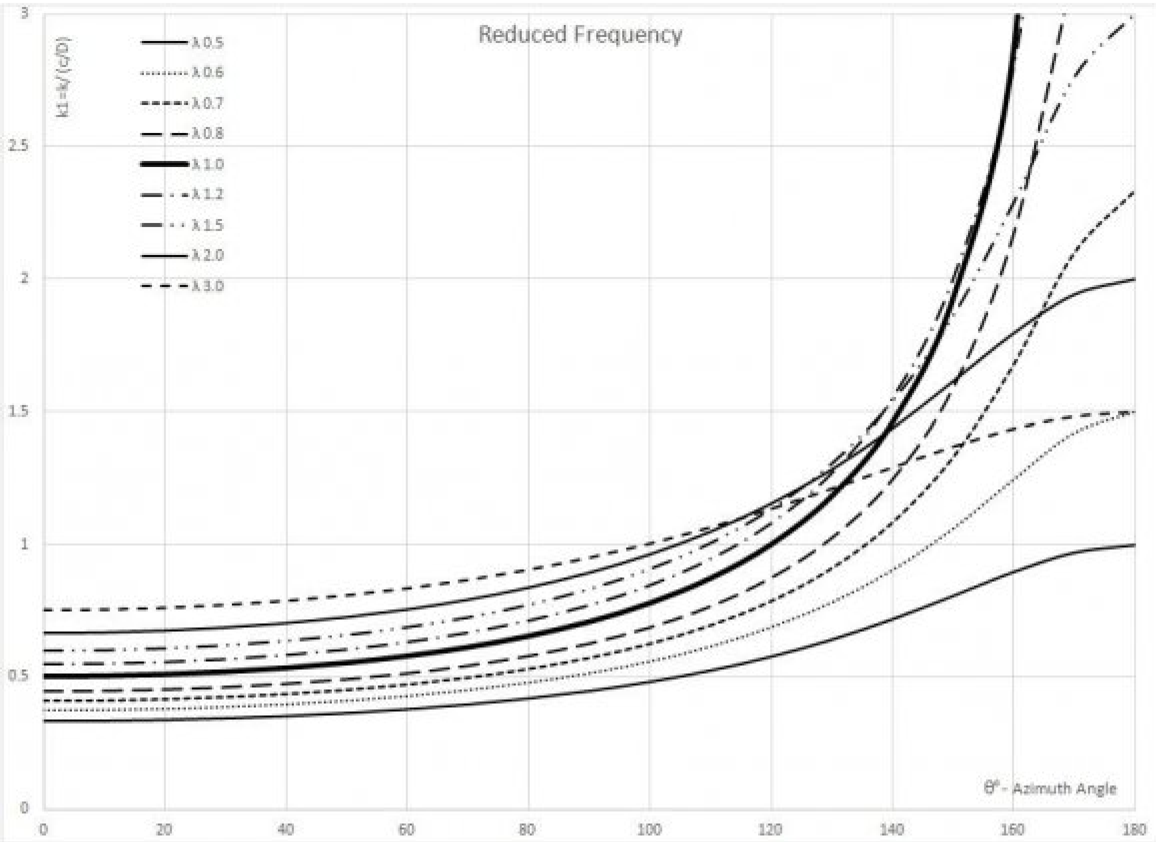

Figure 6: Figure 3 :

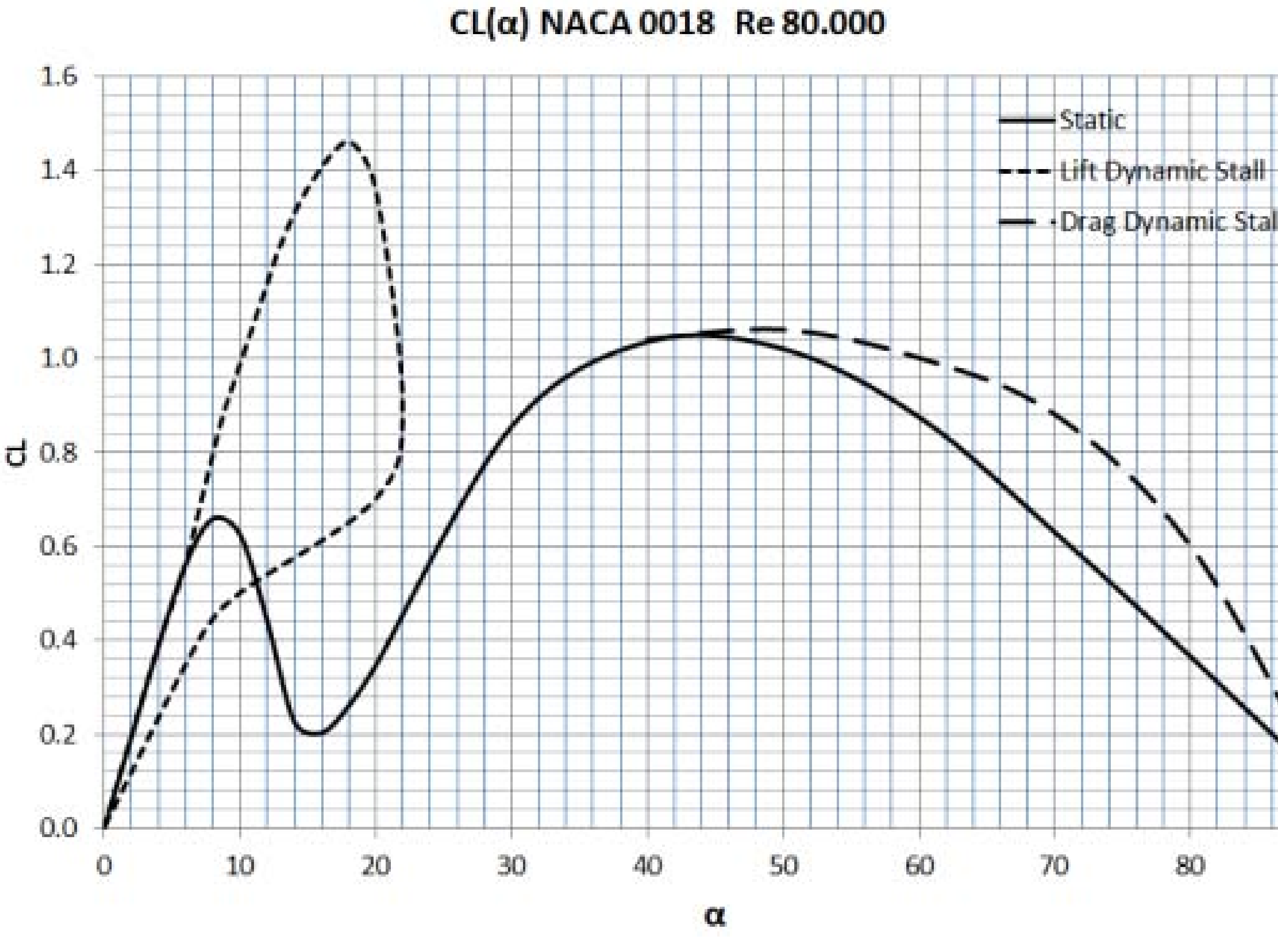

Figure 7: Figure

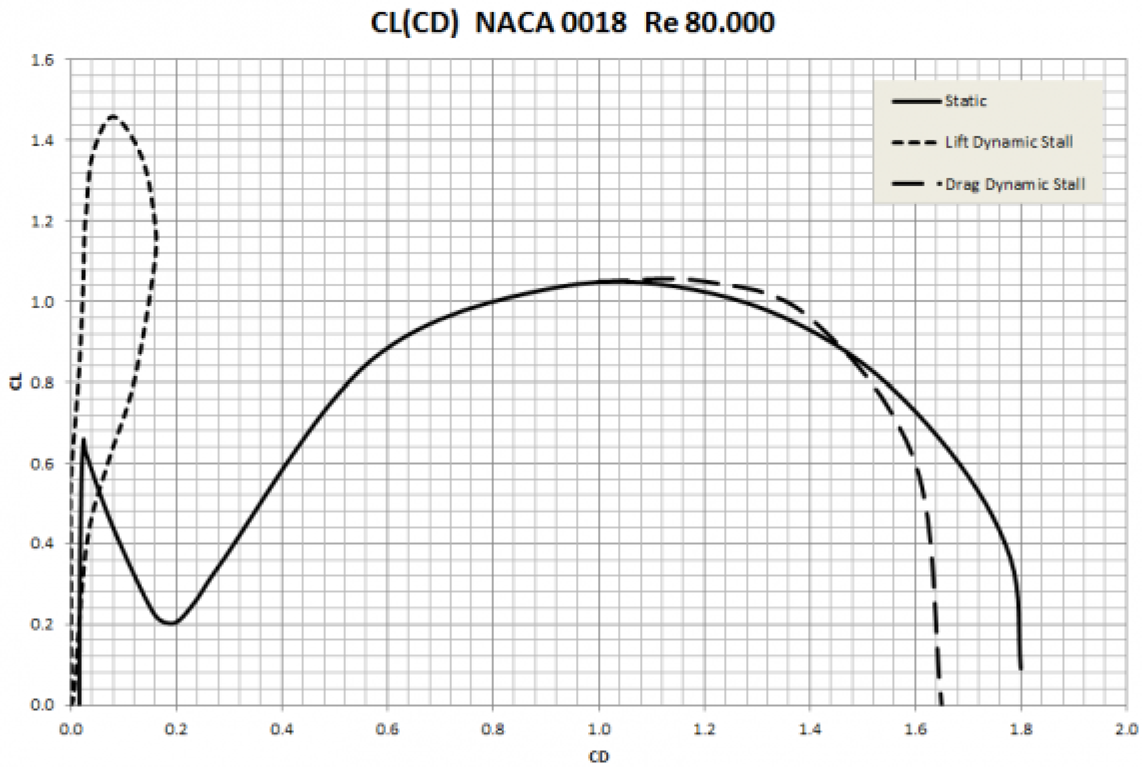

4

Figure 8: Figure 4 :

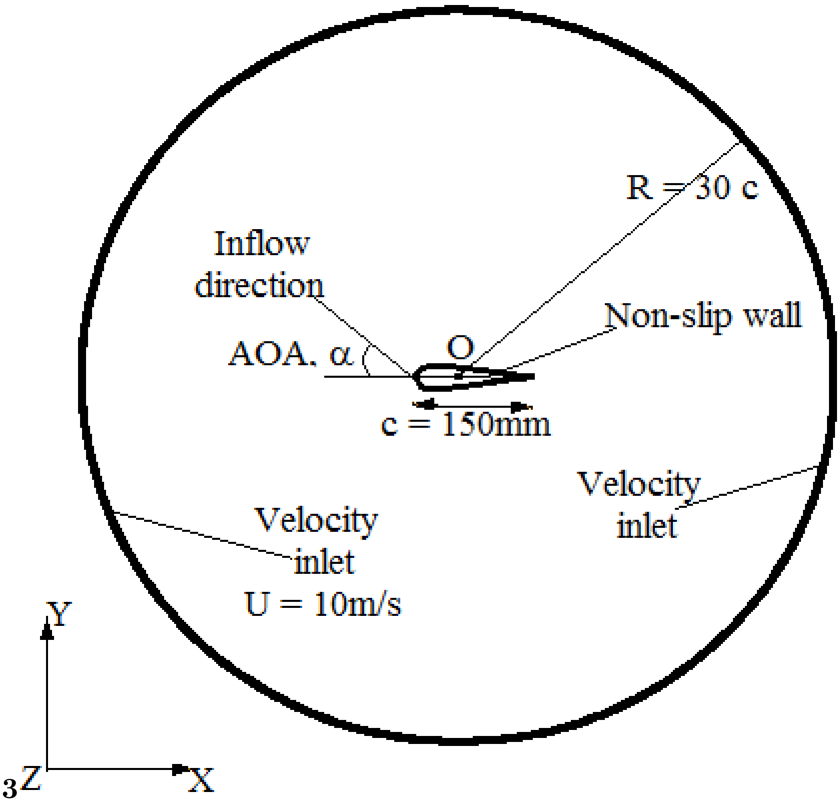

Figure 9: (3)

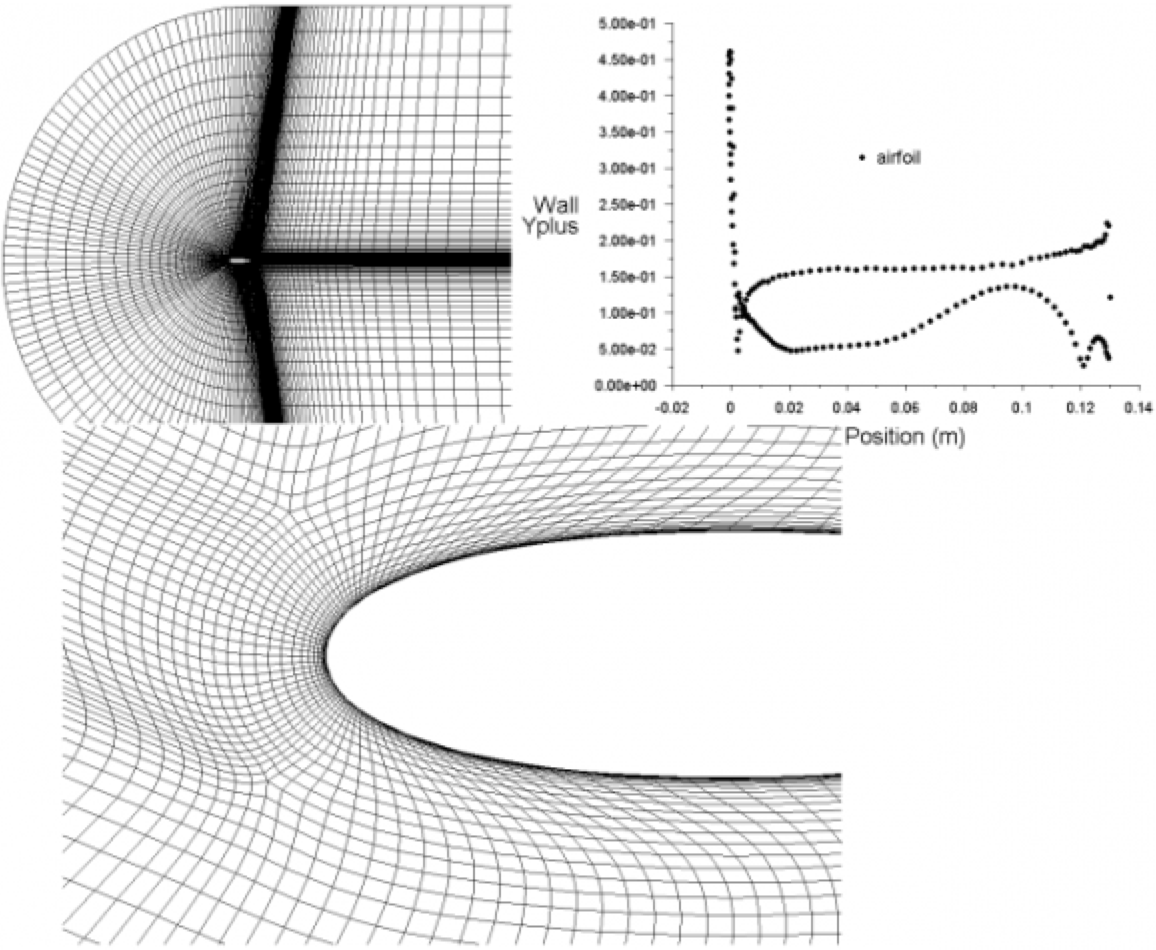

Figure 10: 0

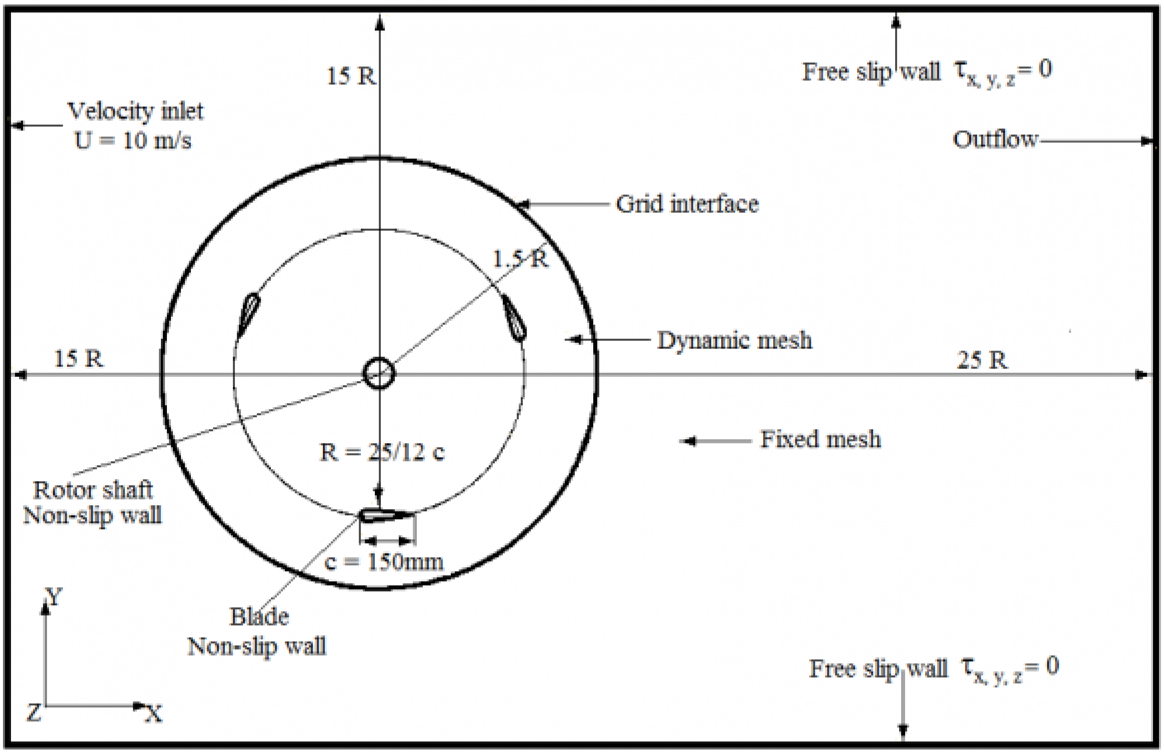

5

Figure 11: Figure 5 :

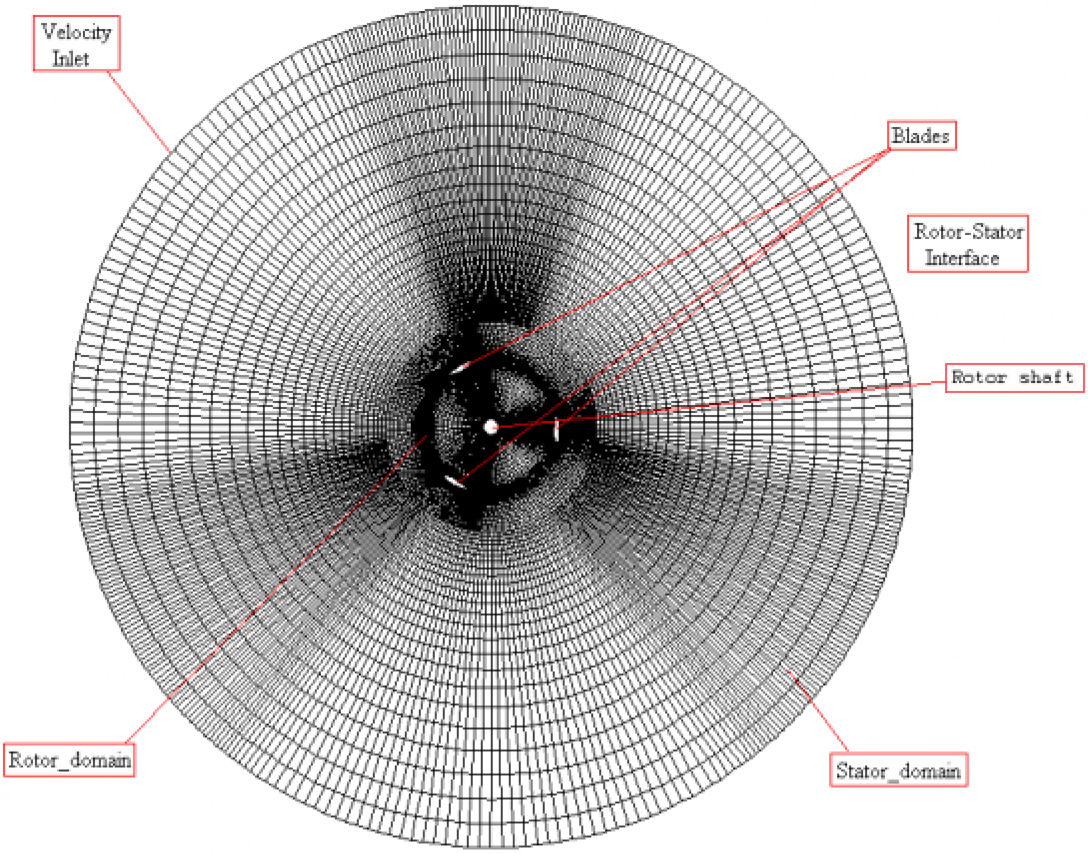

6

Figure 12: Figure 6 :

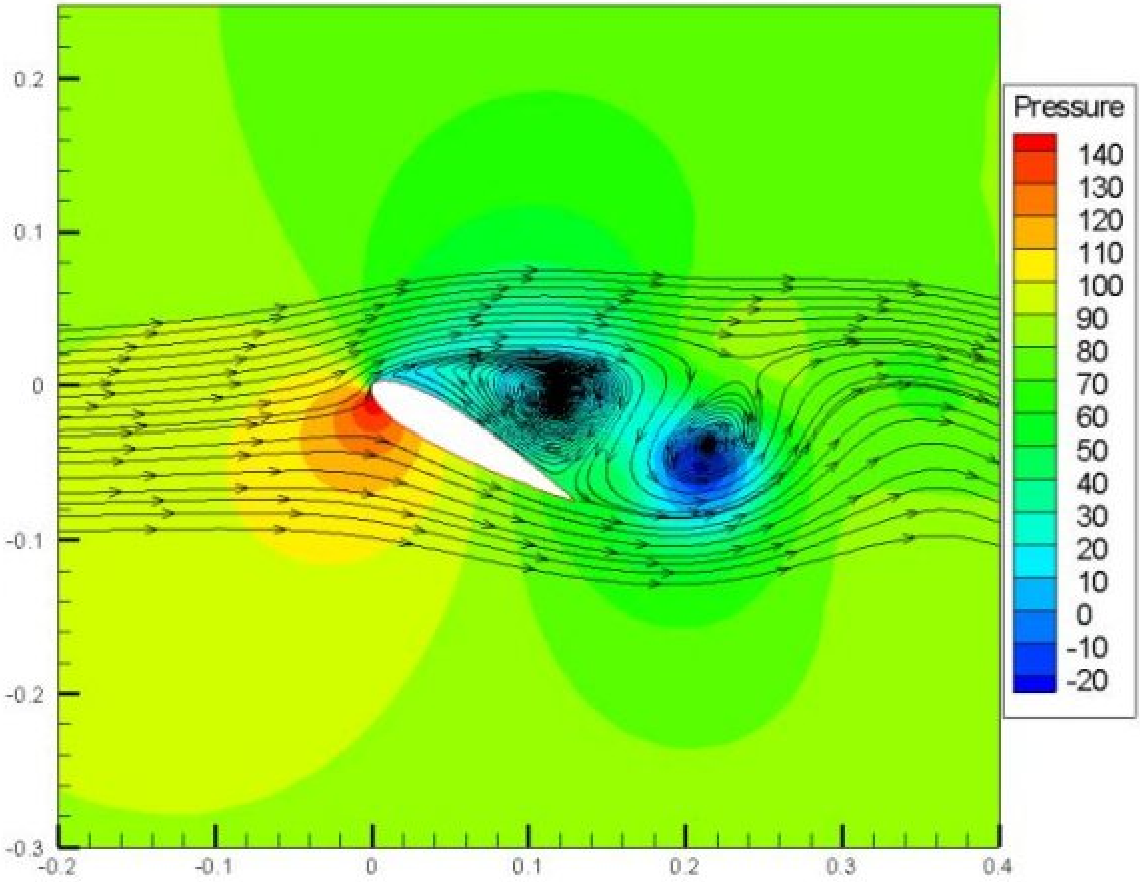

187

Figure 13: 18 IFigure 7 :

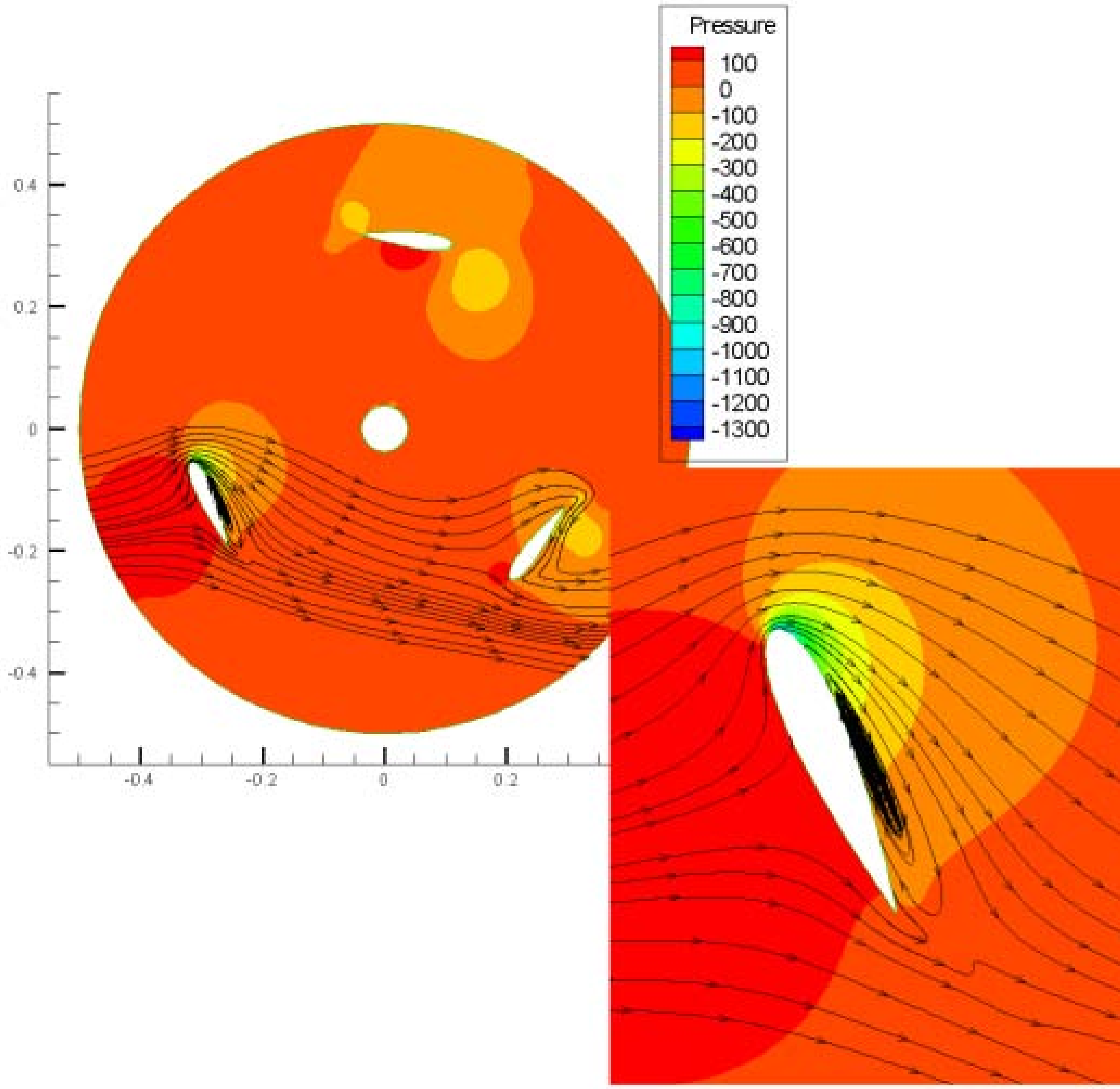

8

Figure 14: Figure 8 :

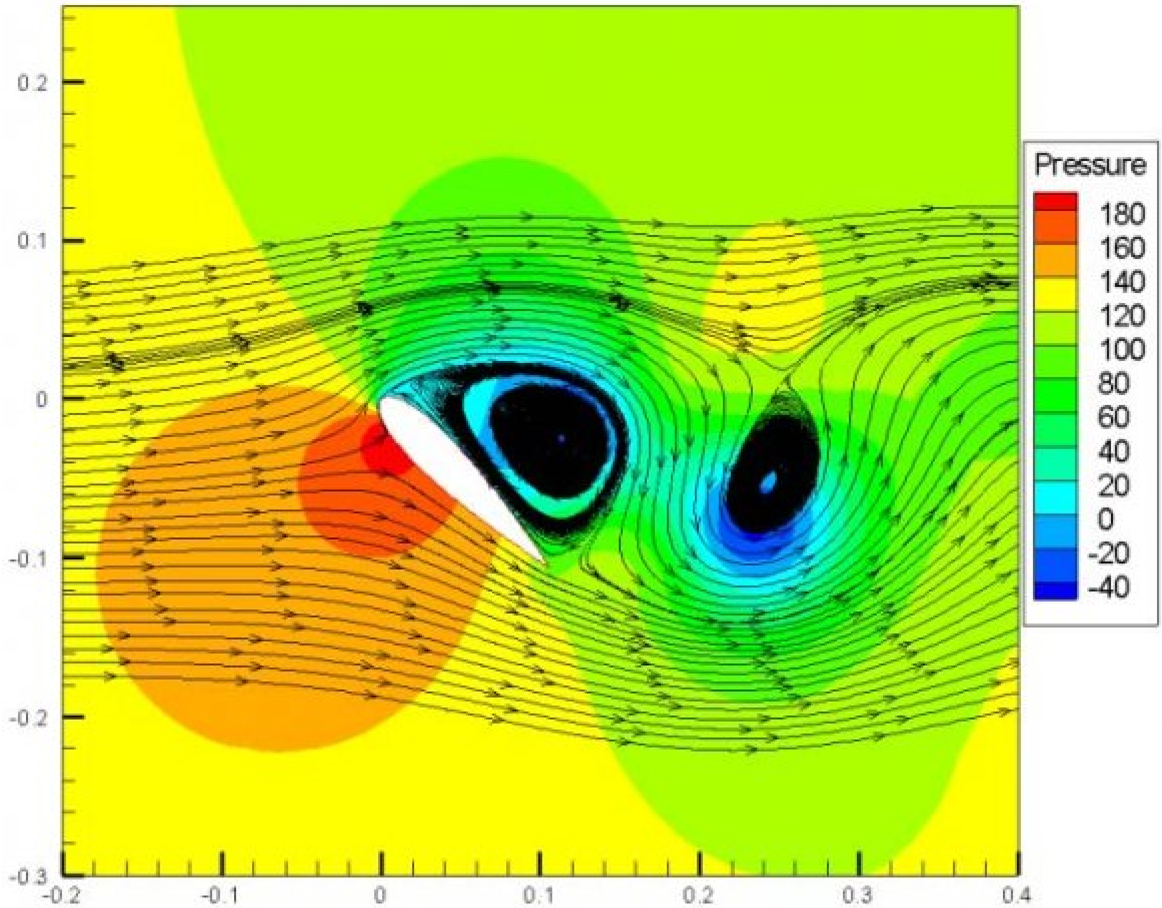
Pressure
180
160
140
120
100
80
60
40
20
0
-20
-40
0.2
0.1
0
-0.1
-0.2
-0.3
-0.2
-0.1
0
0.1
0.2
0.3
0.4

Figure 15:

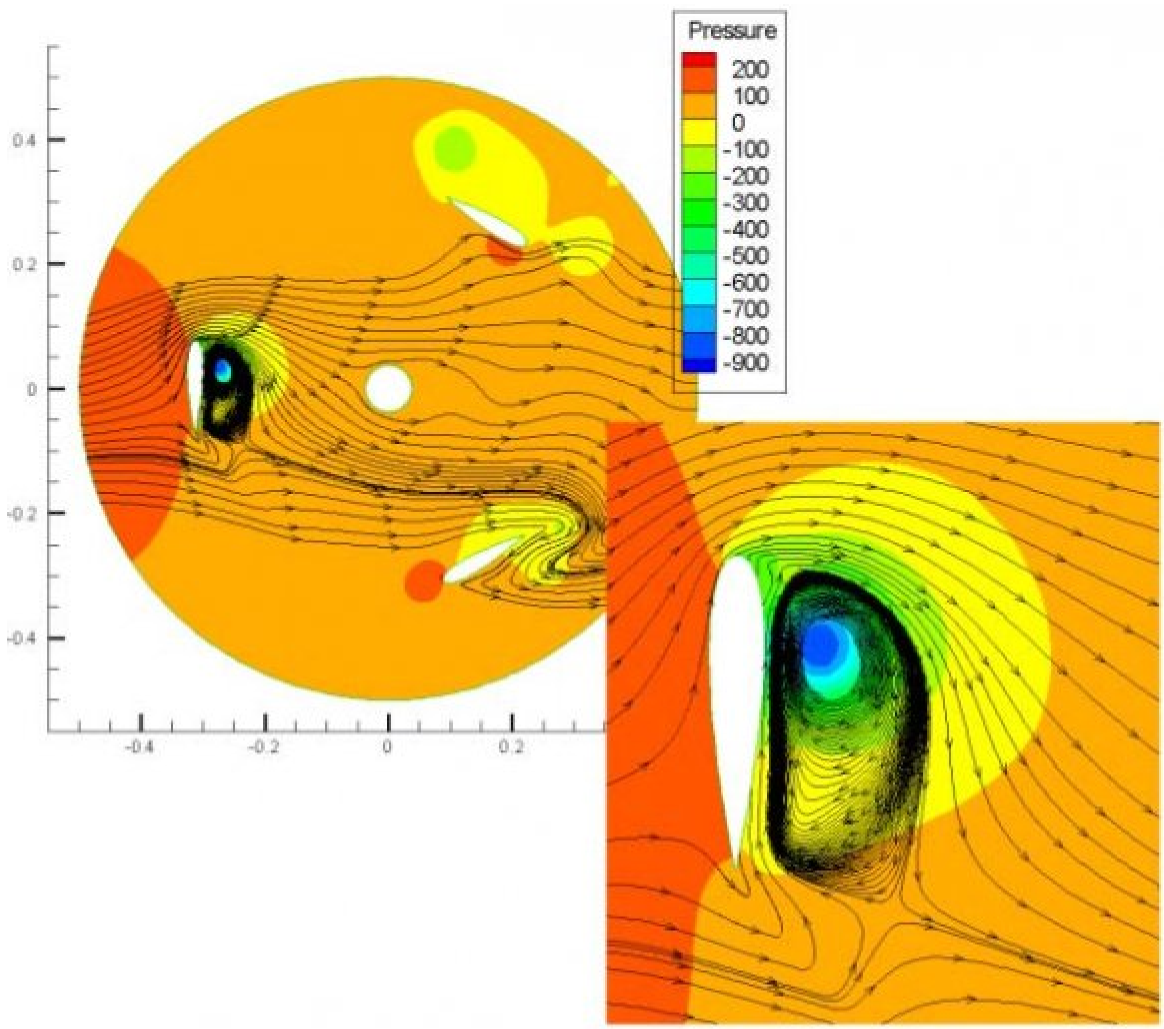

Figure 16:

? 00 45 (22.5) D ? ?
?

actually the so-called laminar separations bubble (LSB) in which the flow turbulence intensity is significantly enhanced and this causes a turbulent boundary layer to appear after the LSB. The LSB grows in size and it travels towards the trailing edge of the airfoil as increases and at the LSB becomes turbulent beginning from the trailing edge. At

Figure 17:

.1 VI.

.2 Aknowledgments

This work was realized through the Partnership programme in priority domains -PN II, developed with support from ANCS CNDI -UEFISCDI, project no. PN-II-PT-PCCA-2011-32-1670.

[Scheldahl R and Limas ()] *Aerodynamic characteristics of seven symmetrical airfoil sections through 180-degree angle of attack for use in aerodynamic analysis of vertical axis wind turbines*, W Scheldahl R , P C Limas . 1981. Albuquerque, NM, USA. Sandia National Laboratories (Tech. Rep. SAND 80-2114)

[Cebeci T et al. ()] *Analysis of low-speed unsteady airfoil flows*, Cebeci T , M Platzer , H Chen , C Chang K , J P Shao . 2005. Germany: Springer.

[Ekaterinaris and Platzer ()] 'Computational prediction of airfoil dynamic stall'. J A Ekaterinaris , M F Platzer . *Progress in Aerospace Sciences* 1997. 33 p. .

[Gao et al. ()] 'Computational study of unsteady flows around dragonfly and smooth airfoils at low Reynolds number'. H Gao , H Hu , J Wang Z . *46 th AIAA Aerospace Sciences Meeting and Exhibit*, (Reno, Nevada) 2008.

[Sørensen N and Michelsen (2004)] 'Drag prediction for blades at high angle of attack using CFD'. N Sørensen N , J A Michelsen . *Journal of Solar Energy Engineering* Nov). 2004. 126 p. .

[Sørensen N and Michelsen (2004)] 'Drag prediction for blades at high angle of attack using CFD'. N Sørensen N , J A Michelsen . *J. Solk. Energy Eng* Nov. 2004. 126 p. .

[Geissler et al. ()] 'Experimental and numerical investigations of dynamic stall on a pitching airfoil'. Werner P Geissler , W Raffel , M Kompenhans , J . *AIAA J* 1996. 34 (5) p. .

[Ingham B et al. ()] Wang S D Ingham B , Ma L , M Pourkashanian , Z Tao . *Numerical investigations on dynamic stall of low Reynolds number flow around oscillating airfoils*, 2010. 39 p. .

[Gharali K and Johnson D ()] 'Numerical modeling of an S809 airfoil under dynamic stall, erosion and high reduced frequencies'. Gharali K , A Johnson D . DOI: 1016/2011.04.037. *Appl. Energy* 2011.

[Allet A et al. ()] 'Numerical simulation of dynamic stall around an airfoil in Darrieus motion'. Allet A , S Halle , Paraschivoiu I . *Journal of Solar Energy* 1999. 121 p. .

[Travin A et al. ()] 'Physical and numerical upgrades in the detached-eddy simulation of complex turbulent flows'. Travin A , M Shur , M Strelets , P R Spalart . *Advances in LES of complex flows*, 2004. p. .

[Carr L ()] 'Progress in analysis and prediction of dynamic stall'. W Carr L . *Journal of Aircraft* 1988. 25 (1) p. .

[Langtry R and Menter ()] *Transition modeling for general CFD applications in aeronautics*, B Langtry R , F R Menter . 2005-522, 2005. AIAA Paper.

[Paraschivoiu I ()] *Wind turbine design with emphasis on Darrieus concept*, Paraschivoiu I . 2002. Montreal: Polytechnic International Press.